Environ. Sci. Technol. **1998**, *32,* 3266−3272

Polycyclic Aromatic Hydrocarbon Contamination in Marine Sediments near Kitimat, British Columbia

CHRISTOPHER D. SIMPSON, CHRISTOPHER F. HARRINGTON, AND WILLIAM R. CULLEN*

Chemistry Department, University of British Columbia, 2036 Main Mall, Vancouver, BC, Canada, V6T 1Z1

DOUGLAS A. BRIGHT† AND KENNETH J. REIMER‡

Environmental Sciences Group, Royal Roads Military College, FMO Victoria, BC, Canada, V0S 1B0

Polycyclic aromatic hydrocarbons (PAHs), like many other hydrophobic organic contaminants, are rapidly sorbed to particles and incorporated within sediments in aquatic systems. The PAH composition within the sediments reflects the source(s) from which the PAHs were derived. However the "source signature" may be altered by postdepositional weathering or biodegradation. In the present study, variation in PAH composition was investigated in size-fractionated sediments and depth-fractionated sediments collected from a Canadian fjord contaminated with aluminum smelter derived PAHs. Multivariate analyses of PAH compositional data consistently showed that different sampling sites could be discriminated on the basis of their PAH composition, but smaller versus larger size fractions within a site could not. The composition of unsubstituted and alkyl-substituted PAHs in a sediment core primarily showed changes with depth that were attributable to enhancement of anthropogenic inputs in the upper core segments. No trends with sediment depth, associated with compound-specific weathering or biotransformation, were noted in the composition of anthropogenically generated PAHs. This may indicate a limited chemical and biological availability of the aluminum smelter derived PAHs.

Introduction

The PAH composition at a given point in the environment reflects the source from which the PAHs were derived; however this "source signature" will be altered by environmental processes which act selectively or differentially on individual PAHs. Thus the change in composition of PAH burden with depth in sediment cores has been explained in terms of changing source inputs over time (*1, 2*), or long-term diagenesis (*3, 4*). Changes in PAH composition as a function of sediment particle size have been attributed to different source inputs (*5*) or differential partitioning among particle size classes (*6, 7*).

* Corresponding author e-mail: wrc@chem.ubc.ca; fax: (604) 822-2847; phone: (604) 822-4435.

† Present address: Applied Research Division, Royal Roads University, 2005 Sooke Road, Victoria, BC, Canada, V9B 5Y2.

‡ Present address: Environmental Sciences Group, Royal Military College, Kingston, Ontario, Canada, K7K 5L0.

Kitimat Arm (Figure 1) is the site of three major industries: an aluminum smelter, a pulp mill, and a methanol-producing plant. Several studies have documented the elevated levels of PAHs in Kitimat Arm and Douglas Channel due to inputs from the aluminum smelter, which operates eight potlines, and utilizes vertical stud Söderberg electrodes (*8*−*10*). Smelters of this design are known to release substantial amounts of PAHs to the receiving environment because of pyrolysis and volatilization of the pitch/tar anode binder from the Söderberg electrode, and from the handling of pitch and coke on site (*11, 12*).

This paper provides an evaluation of the fate of unsubstituted and alkyl-substituted PAH inputs from an aluminum smelter to sediments of a fjord along the British Columbia coast. Information is presented on the distribution of individual PAHs among five different sediment size fractions, as well as on changes in composition with depth in sediments associated with both diagenesis and the onset of anthropogenic activities in Kitimat Arm.

Experimental Section

Surface sediment samples (∼15 cm depth) were collected from seven sites in Kitimat Arm, Douglas Channel, British Columbia (Figure 1), by using either a stainless steel Smith-McIntyre or Petite Ponar grab sampler. Three samples from each site were collected, pooled, and mixed thoroughly, and the subsamples transferred to 1-L precleaned, oven-baked amber glass bottles. The samples were immediately frozen (−20 °C) and later transported back to the laboratory. The pooling of triplicate grab samples at each site helped to minimize within-site variability.

A sediment core was collected in Giltoyees Inlet (Figure 1). The 9.0-cm-diameter gravity corer consisted of a 122-cm-long polyacrylic tube mounted at one end in a weighted aluminum alloy head, and fitted with a stainless steel cutter/catcher at the other. The core was subsectioned vertically into 5-cm slices, which were wrapped in baked aluminum foil, frozen at −20 °C, and transported back to the laboratory.

All surface sediment samples (i.e., not including core segments) were freeze-dried and then dry sieved through brass sieves into the following size fractions: >1180 μm, 1180−300 μm, 300−180 μm, 180−38 μm, <38 μm. The methodology used for the analysis of unsubstituted PAHs in the surface sediment samples has been previously described in detail and validated by the use of standard reference materials (*13*). Briefly, PAH concentrations in surface sediment samples were determined by GC-FID on a Hewlett-Packard 5890 GC equipped with a split/splitless injector, 30-m FSOT PTE-5 GC column (Supelco Ltd.; 0.32-mm internal diameter, 0.25-μm stationary phase) and a flame ionization detector (FID), after Soxhlet extraction with methylene chloride of a subsample (10−20 g) of freeze-dried sediment. Hexamethylbenzene was used as a quantitation standard and was added to the sediment aliquot prior to extraction. The minimum detectable concentration (defined for each sample as the concentration of analyte that would give rise to the minimum peak area which could be distinguished from the background by the integration software used) was typically 50−200 ng/g, and varied from sample to sample as a function of the total amount of extractable material present in each sample. Trace amounts of naphthalene (typically ∼0.4 ng) were detected in blank extracts, but none of the other PAHs were ever detected in blank extracts. Method validation studies (*13*) determined a standard error of less than ±15% for replicate injections of a single extract, and ca.

S0013-936X(97)00419-7 CCC: $15.00
Published on Web 09/10/1998

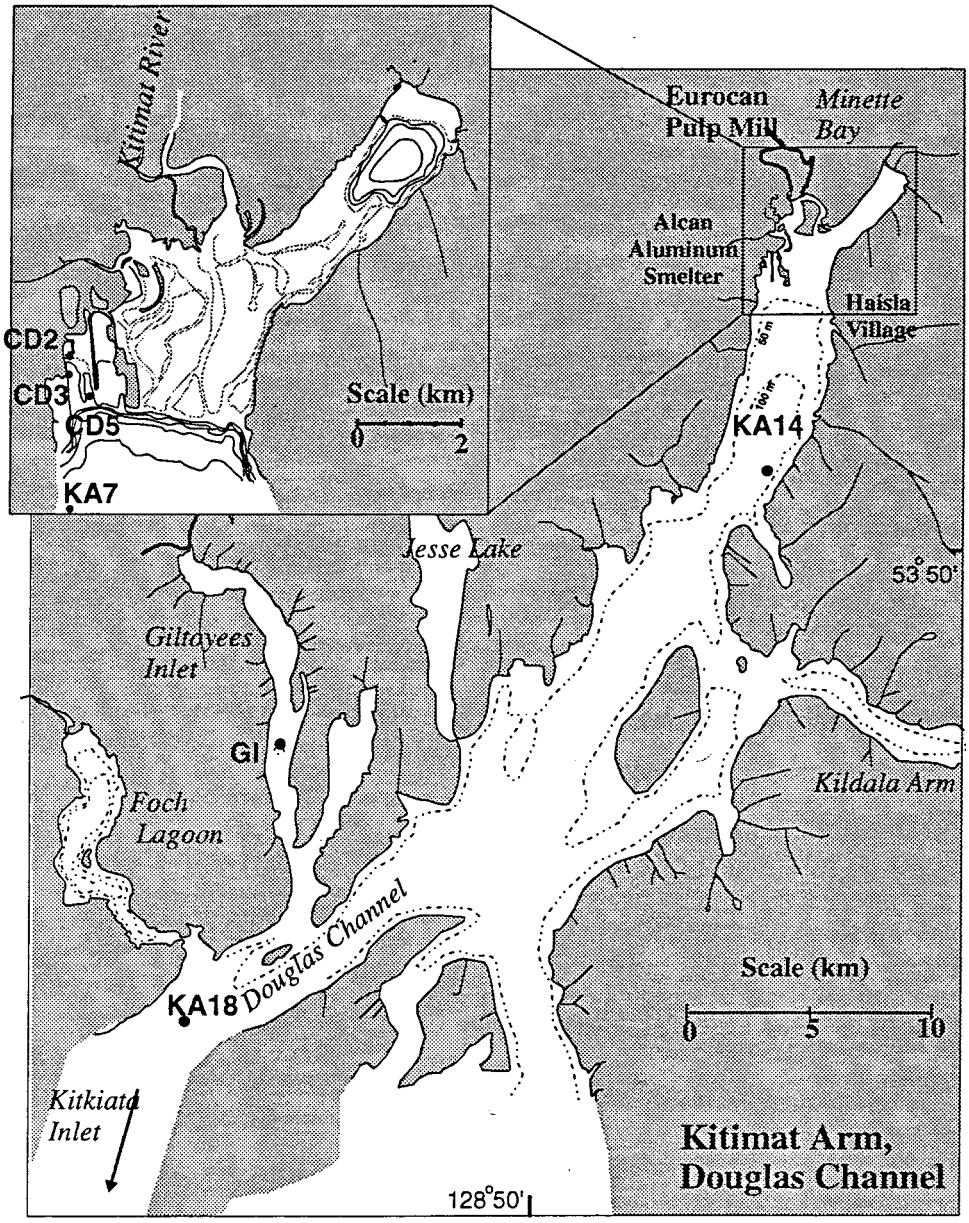

FIGURE 1. Map of Kitimat Arm/Douglas Channel fjord system illustrating sample locations.

±30% for independent analyses from a single site. Recovery of the hexamethylbenzene standard was 85 ± 17%.

The sediment core samples were to be analyzed for both unsubstituted PAHs and selected alkylated PAH homologues. The methodology, described in the preceding section and applied to the surface sediment samples, did not provide adequate sensitivity or compound specificity required for the analysis of the sediment core sections. Therefore analysis of the core for a suite of unsubstituted and alkylated PAH (see Table 2) was undertaken by a commercial laboratory (Axys Analytical Services Ltd., Sidney, BC), using a GC−MS-based protocol, as described by Yunker et al. (*14*). PAH concentrations were determined in core segments by GC−MS (Finnigan Incos 50 mass spectrometer, Varian 3400 gas chromatograph, CTC autosampler, and a DG 10 data system), after sequential extraction of the dried sediment extract with methanol, and then methylene chloride. The GC was fitted with a DB-5 column (30 m, 0.25 mm i.d. x 0.25 μm film thickness), and the mass spectrometer was operated in the electron impact (EI) mode (70 eV) using multiple ion detection, acquiring two characteristic ions for each target analyte and surrogate standard. The marine reference standard HS6 (National Research Center, Canada) certified for PAHs, was also analyzed to ensure the validity of this method.

Principal Components Analysis (PCA) was performed on the PAH compositional data for samples from seven sites × five size fractions (n = 35) by using SYSTAT 5.0. Prior to analysis, nondetected values in the data set were replaced with random numbers between zero and the sample-dependent minimum detectable concentration. This was done to ensure the PCA was not influenced by spurious correlations between compounds that were undetected at some sites. The data for individual compounds was then normalized to the total PAH concentration for each sample to remove the effect of differences between sites in absolute PAH concentration.

Results and Discussion

Distribution of PAHs among Particle Size Classes in Surficial Sediments. PAH concentrations for each sediment size fraction from the seven sites are listed in Table 1. The size distribution of sediment particles at each site is also included

TABLE 1. PAH Concentrations (ng/g, dry sediment) in Various Size Fractions of Kitimat Surface Sediments[a]

Fraction, μm	wt %	naph	acen	acny	flu	phen	anth	fln	pyr	chry	Baa	Bxf	Bep	Bap	Pery	ipyr	dib	bper	∑ PAH
CD2																			
>1180	3	16184	<10	27 073	15 800	165 188	39 196	367 027	341 583	243 731	290 915	326 937	331 141	449 749	118 000	371 668	112 134	360 248	3 576 574
1180−300	8	16121	<10	15 467	8 852	85 435	19 438	163 008	146 917	101 723	111 144	268 751	121 837	158 585	42 000	147 371	41 046	145 490	1 593 184
300−180	22	3086	19	3 545	2 194	21 257	4 732	41 484	37 155	25 885	29 984	74 656	35 169	46 559	12 700	57 645	15 406	53 584	465 060
180−38	49	1295	<10	1 270	789	7 997	1 631	16 466	14 706	10 519	12 865	28 489	11 365	17 468	5 250	18 105	5 290	17 940	171 443
<38	18	320	<10	347	219	2 388	451	5 497	5 001	3 372	4 644	11 358	5 561	6 038	2 250	7 786	2 244	7 191	64 667
CD3																			
>1180	5	41	<10	17	<10	125	32	631	658	488	618	1 322	766	1 091	560	1 084	229	1 047	8 709
1180−300	8	514	<10	322	174	1 252	270	2 505	2 228	1 650	2 246	4 082	2 270	3 122	1 950	2 915	901	2 683	29 082
300−180	16	168	<10	122	59	495	112	1 036	920	613	800	1 274	804	1 125	2 440	1 196	457	1 320	12 940
180−38	50	78	<10	21	13	104	22	216	198	148	211	317	196	278	1 340	213	74	230	3 658
<38	23	68	<10	6.1	7.9	36	5.7	81	74	85	119	164	104	213	2 360	132	68	203	3 727
CD5																			
>1180	14	45	<10	20	18	71	11	162	177	167	135	198	162	125	40	106	50	173	1 661
1180−300	32	40	<10	22	19	69	10	142	146	168	133	182	172	133	50	129	117	124	1 656
300−180	26	79	<10	25	20	78	11	175	175	174	146	183	168	172	50	54	56	143	1 708
180−38	17	37	<10	7.1	16	87	9.4	188	190	172	156	250	155	148	50	117	48	169	1 798
<38	11	39	<10	5.7	15	50	10	95	116	122	99	148	108	96	30	78	54	103	1 169
KA7																			
>1180	5	212	<10	177	113	1 127	252	2 207	2 155	1 465	2 026	2 150	1 997	2 439	730	2 104	586	2 013	21 753
1180−300	47	886	<10	277	330	2 080	401	4 279	4 135	3 007	3 991	2 014	2 168	3 285	990	2 706	473	2 526	33 549
300−180	0	1131	<10	33	51	373	56	788	828	667	1 053	1 814	837	1 540	120	833	446	950	11 521
180−38	26	190	<10	146	102	1 011	200	2 052	2 011	1 345	1 815	1 993	1 225	1 768	580	1 690	496	1 443	18 068
<38	22	135	<10	35	44	269	61	598	588	498	698	481	492	616	230	497	91	489	5 821
KA14																			
>1180	36	50	<10	28	6.1	145	34	289	294	277	249	532	261	293	140	323	129	400	3 450
1180−300	31	58	<10	36	6.8	151	36	305	325	277	259	545	264	290	130	273	100	310	3 368
300−180	8	67	<10	25	16	138	32	267	300	264	267	516	258	297	130	259	109	337	3 284
180−38	15	55	<10	27	27	173	38	332	332	273	299	555	269	330	140	284	99	333	3 566
<38	10	76	<10	24	6.7	130	18	280	311	233	241	542	269	332	130	294	111	294	3 292
KA18																			
>1180	42	89	<10	11	26	85	<10	119	156	267	206	195	129	167	110	212	128	154	2 055
1180−300	42	86	<10	<10	27	82	<10	119	177	300	256	232	148	136	170	132	73	187	2 125
300−180	6	169	<10	35	29	104	<10	160	227	276	206	263	171	209	100	161	101	177	2 387
180−38	8	127	<10	20	24	103	<10	141	181	264	162	199	141	182	80	140	111	158	2 034
<38	2	430	<10	21	31	107	<10	136	168	264	94	261	169	635	60	133	124	156	2 791
GI																			
>1180	7	106	<10	15	26	46	26	142	265	314	135	230	235	203	150	210	170	162	2 435
1180−300	40	76	<10	<10	19	28	13	78	125	217	54	113	128	81	90	63	67	113	1 263
300−180	26	87	<10	<10	16	22	13	71	113	192	45	111	105	69	80	100	175	135	1 335
180−38	21	88	<10	<10	17	32	12	80	115	208	52	134	123	107	100	304	448	195	2 015
<38	7	120	<10	<10	14	38	11	79	127	156	49	115	114	105	60	162	181	126	1 458

[a] Abbreviations: naph, naphthalene; acen, acenaphthene; acny, acenaphthylene; flu, fluorene; phen, phenanthrene; anth, anthracene; fln, fluoranthene; pyr, pyrene; chry, chrysene; Baa, benzo[*a*]anthracene; Bxf; benzofluoranthenes; Bep, benzo[*e*]pyrene; Bap, benzo[*a*]pyrene; Pery, perylene; ipyr, indeno[1,2,3-*c,d*]pyrene; dib, dibenz[*ah*]anthracene; bper, benzo[*ghi*]perylene; ∑PAH, sum of 17 PAHs listed in Table 1; wt %, fraction of total sediment weight accounted for by a given sediment particle size range.

in Table 1. An examination of the absolute PAH concentration in each sediment size fraction (Table 1) suggests obvious differences between size fractions only for the inner harbor sites CD2 and CD3, where individual PAHs (except perylene at CD3) were enriched in the larger particle size fractions. Correlations between increasing median particle size and higher PAH levels were statistically significant for site CD2 ($r = 0.98$; $P = 0.0023$), but not for any other site ($P \geq 0.22$ for all). For sites other than CD2 and CD3, individual and total PAH concentrations were similar in all size fractions or exhibited only slight variation with no apparent pattern. Enrichment of PAHs in specific particle size classes has been reported previously in marine sediments (*5*, *6*). Prahl and Carpenter (*5*) determined that PAHs in coastal marine sediments near Washington State were selectively associated with a low density, large particle size sediment fraction (>64 μm) which they suggested comprised mainly vascular plant remains and pieces of charcoal. Maruya et al. (*6*) noted a correlation between PAH content and the abundance of silt and clay in San Francisco Bay sediments, but the correlation between PAH and organic carbon content of the sediments was poor. They ascribed these observations to a heterogeneity of organic carbon matrixes, and specifically, to aromatic-rich soot particles in the silt/clay fraction, which strongly bind PAHs. In a previous paper (*8*), the relationship between PAH concentration and sediment organic carbon (f_{OC}) was investigated for sediments collected from the Kitimat fjord system. It was suggested that after deposition into the environment PAHs remained associated with the carbonaceous particles to which they were bound when initially introduced into the environment. In these sediments, there was no evidence of equilibrium-driven partitioning to f_{OC}; therefore f_{OC} measurements on size-fractionated sediments were not included in the present study.

The major sources of PAHs to Kitimat Arm are expected to be atmospheric particulate emissions, aqueous effluents, and spillage of raw materials (coke briquettes, pencil pitch) from the aluminum smelter. The preferential association of PAH with larger particle sizes at the inner harbor sites (CD2 and CD3), the very high absolute PAH concentrations (especially at CD2), and the striking similarity in PAH composition between smelter feedstocks and harbor sediments (*15*) strongly suggest that raw material spillage is the dominant PAH input affecting sites CD2 and CD3. In contrast, the uniform PAH distribution among size-fractionated sediments from the other locations (CD5, KA7, KA14, KA18, and GI1) may indicate that PAHs derived from sources other than raw material spillage may be more important for these sites.

The PAH composition at CD3 is sharply different from all other sites—especially in the smaller size fractions where perylene becomes the dominant PAH. If perylene is ignored, however, the composition in all size fractions at CD3 is almost identical with CD2. We also observed that the distribution of retene (1-methyl-7-isopropylphenanthrene) in all extracts from CD3 correlated significantly with perylene ($r = 0.93$, $P = 0.02$), and poorly with all other PAHs ($P > 0.43$) (data not shown). Retene was not detected in coke briquettes or pencil pitch from the aluminum smelter, and combustion or pyrolysis of these fossil fuels would not be expected to result in formation of retene.

The presence of both retene and perylene in marine sediments has often been attributed to early diagenesis of organic matter (*1*, *16*, *17*). In the case of retene, which is thought to be formed through degradation of abietic acid (*1*, *17*) and is often present in sediments impacted by runoff from coniferous forests (conifers are the dominant flora in the Kitimat catchment), the organic matter undoubtedly has a terrestrial source. Therefore the close coupling between retene and perylene at CD3 (and the accompanying poor correlation with other PAHs) indicates a recent terrestrial origin for these compounds. Thus we conclude that the PAH composition at CD3 is the result of mixing of smelter-derived inputs, which dominated the large particle size fractions, and PAHs derived from terrestrial organic matter (retene, perylene), which dominate the small particle size fractions.

Differential partitioning of PAHs among sediment particle size classes could also affect the composition of the PAHs mixture in these sediments. The composition of PAHs in individual samples representing five different size fractions and six different sites was examined by using principal components analysis (PCA). PCA allows the exploration of similarities or differences between samples based on complex compositional data, and is often applied to assist with the interpretation of environmental chemistry data (*14*, *18*). The intersample variation in concentrations of the 16 individual PAHs is "captured" onto a reduced set of principal components, which are linear combinations of the original variables.

The PCA analysis was run initially with all data shown in Table 1, but PAH data from site CD3 were subsequently excluded. The perylene-rich PAH composition of all size fractions of the sample collected from CD3, especially the finer fractions, set them apart from all other samples. The first two principal components (PC1 and PC2) captured 34.7% and 20.2% of the between-sample variation in the original data set.

The proximity of individual samples to each other in Figure 2 reflects their compositional similarity. The five particle size classes are coded in the figure as 1 to 5 (e.g., CD5-*5*), from the largest to the smallest size fraction. There was no apparent grouping of the samples on the basis of similarities in particle size for any of the first four principal components. The PAH composition instead reflects the geographic location of the collection sites. The sites are distributed along PC1 according to their proximity to the head of Kitimat Arm, with samples (all size fractions) from Giltoyees Inlet (site GI) and KA18 plotting to the left of the origin. Some separation between different sites is also evident on PC2: Site CD2 is distinguishable from CD5 on the basis of the PAH composition, with sites KA7 and KA14 forming an intermediate, semidiscrete group. Similar site groupings were evident when the dataset was subjected to cluster analysis.

The influence of specific PAHs on multivariate similarities or differences between samples is indicated by the component loading for each variable. PC1 was positively correlated with component loadings for phenanthrene, fluoranthene, benzo[*a*]anthracene, and benzofluoranthenes and was negatively correlated with naphthalene, fluorene, chrysene, perylene, and dibenz[*ah*]anthracene. PC2 was positively correlated with component loadings for fluorene and pyrene and negatively correlated with indeno[1,2,3-*cd*]pyrene and benzo[*ghi*]perylene. (Benzo[*e*]pyrene, benzo[*a*]pyrene, and acenaphthylene were not significantly correlated with either PC1 or PC2, $P \geq 0.05$).

The PCA reflects, above all, a different PAH composition at sites proximate to the smelter compared to sites further removed from it. This is consistent with the reduced importance of aluminum smelter derived PAH inputs relative to naturally occurring PAHs, at the distant sites, as reported previously (*8*).

Influence of Sediment Diagenesis on PAH Composition in Giltoyees Inlet. The concentrations of unsubstituted and alkylated PAHs, and sediment percent organic carbon, in the Giltoyees Inlet core are listed in Table 2. Organic carbon content was highest in the surface sediments, with minimal changes with depth below ~15 cm. The elevated organic carbon in the surficial sediments may reflect increased organic matter inputs in recent times because of logging activity in the Giltoyees watershed. Alternatively, the change

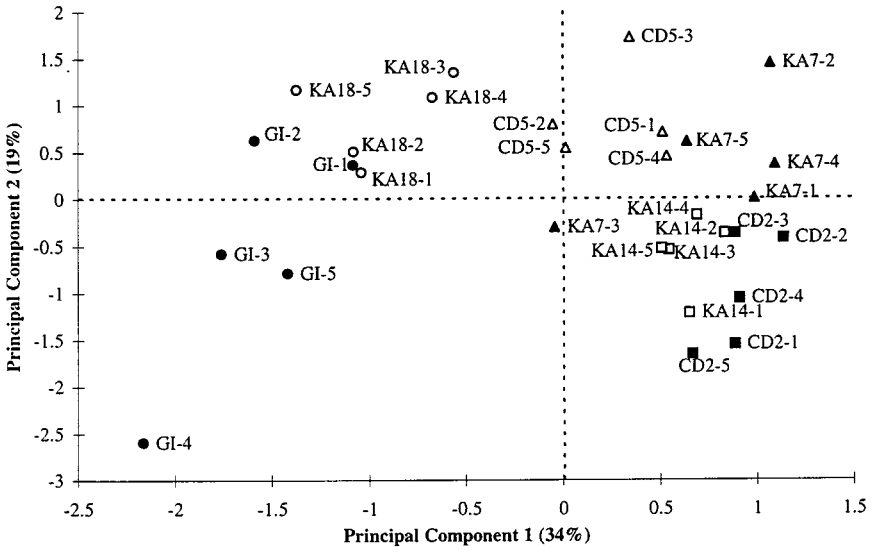

FIGURE 2. Principal components analysis of PAH composition across sites and different particle size fractions (legend: 1, >1180 μm; 2, 300−1180 μm; 3, 180−300 μm; 4, 38−180 μm; 5, <38 μm).

in organic carbon over the top 15 cm may be attributable to microbial breakdown of detrital organic matter in the surficial sediments.

Total PAH concentrations were highest in the top segments of the core, and declined dramatically with depth. Below a depth of 45 cm total PAH levels remained relatively constant. The PAH composition also changed dramatically with depth. The upper 20 cm was dominated by unsubstituted PAHs of intermediate and high molecular weight. The profile is very similar to the contaminated surface sediments discussed earlier in this paper and is attributed to anthropogenic combustion inputs—arising primarily from the aluminum smelter at Kitimat. The core sediments were not dated; however, if one assumes that the sudden increase in PAH concentrations at a depth between 20 and 45 cm coincides with the commencement of operations at the aluminum smelter in 1954, and the effects of sediment compaction and biological mixing are ignored, an approximate sedimentation rate of 0.25−0.5 cm per year is estimated. This is well within the range of values calculated for recent uncompacted sediments in the Kitimat fjord system (*19*). Other workers have reported subsurface maxima in PAH concentrations, coincident with a worldwide reduction in coal combustion and improved emission control technology (*20*−*22*). The lack of a subsurface maxima in the present data supports our contention that the PAH flux at this site is dominated by (ongoing) local inputs.

The PAH composition in core segments below 45 cm is accounted for almost entirely by unsubstituted and alkylated forms of naphthalene, phenanthrene, and pyrene and unsubstituted chrysene and perylene. Many of these compounds have been previously reported in PAH assemblages arising from early diagenesis of plant material (*1*, *2*, *5*, *17*). The major downward trend in the upper core is progressive dilution of the smelter-derived PAH mixture by the natural PAH signature. This is especially evident in the higher relative amounts of naphthalene, phenanthrene, and perylene in the older sediments (Table 2).

Recent studies (*23*, *24*) have suggested that rates of PAH biodegradation in aerobic environments are influenced by the degree of alkylation: More highly alkylated forms tend to be more recalcitrant to weathering, but more susceptible to photooxidation when compared to less highly alkylated species (*25*, *26*). Processes such as these which act differentially upon individual PAHs, will alter the PAH composition. The data in Table 2 were examined for evidence of postdepositional changes in PAH composition. In addition, to explore postdepositional changes in the *anthropogenically enhanced PAHs specifically*, we attempted to remove the contribution of natural inputs from anthropogenically enhanced PAHs. This was done by calculating for each PAH the average concentration in samples below 45 cm depth, and subtracting this from PAH levels in more recent sediments.

Levels of C2 and C3 naphthalenes are highest in recent sediments (upper 10 cm). This indicates that C2 and C3 naphthalenes are derived from anthropogenic inputs, and their absence in older sediments (deeper than 10 cm) simply reflects decreasing anthropogenic inputs with increasing sediment depth. (C1, C2, and C3 alkyl homologues of naphthalene, phenanthrene/anthracene, and fluoranthene/pyrene are present in pencil pitch and coke briquettes used at the aluminum smelter (*15*)). For sediment depths greater than 10 cm, any changes seen in the ratios of alkyl-substituted naphthalenes to unsubstituted naphthalenes, C1 naphthalenes to C2 naphthalenes, or 1-methylnaphthalene to 2-methylnaphthalene, based on either data corrected for natural inputs or the original data, were primarily an artifact of the data being at or below the detection limit in core samples below 10 cm depth.

The absolute concentrations of all phenanthrene alkyl homologue groups were highest in the top 20 cm, indicating significant anthropogenic inputs of these compounds. As was observed for the naphthalene series, there was a general decline in the proportion of C2 phenanthrenes and anthracenes below 10 cm in depth. Retene accounted for the entire C4 anthracenes/phenanthrenes concentration at all depths. The *proportion* of retene increased with increasing depth over the first 20 cm, coincident with decreasing levels of anthropogenic PAHs. However, absolute amounts of retene decreased with depth in the top portion of the core and were constant below 20 cm. The constant retene concentration in the lower core implies that there is no net postdepositional production or degradation of retene in deep sediments, whereas the trend of higher retene concentrations in the upper core suggest an increased flux of retene to recent Giltoyees Inlet sediments, probably related to logging activities in the watershed.

Long-term diagenesis—as in coal or oil maturation, for example—is often characterized by an initial increase in the ratio of alkylated phenanthrenes to phenanthrene, accompanied by a progressive enrichment of the more ther-

TABLE 2. PAH Concentrations (in ng/g, dry weight) in 5-cm Sections from a Giltoyees Inlet Core

	depth in sediment (cm)								
	0–5	5–10	10–15	15–20	45–50	50–55	55–60	60–65	65–70
% organic carbon	1.31	1.02	0.84	0.82	0.81	0.83	0.84	0.80	0.78
compounds									
naphthalene	25	16	4.5	5.2	3.6	7[a]	7.6	13[a]	6.4
acenaphthylene	0.4[a]	0.3	0.28[a]	0.16[a]	<0.12	<0.14	<0.16	<0.19	<0.15
acenaphthene	3.0	3.0	0.38[a]	<0.17	<0.26	<0.18	<0.19	<0.2	<0.33
fluorene	4.0	2.0	0.67	0.25	0.27[a]	<0.25	0.35[a]	<0.28	<0.33
phenanthrene	24	20	5.1	1.7	1.3	1.4	1.3	1.2	1.2
anthracene	5.0	5.0	0.93	0.17[a]	<0.15	<0.17	<0.18	<0.17	<0.18
fluoranthene	66	54	12	2.5	0.22[a]	0.36[a]	0.41[a]	0.24	0.43
pyrene	59	54	14	4.1	1.0[a]	0.97[a]	0.8[a]	0.73	0.88
benzo[*a*]anthracene	30	28	6.4	1.2	<0.21	<0.23	<0.24	<0.23	<0.21
chrysene	50	39	8.4	1.6	0.64	0.36[a]	0.64[a]	0.53	0.5
benzofluoranthenes	170	170	35	7.6	0.65[a]	0.75[a]	<0.28	<0.26	<0.23
benzo[*e*]pyrene	69	68	16	3.1	<0.26	<0.29	<0.3	<0.28	<0.25
benzo[*a*]pyrene	55	50	9.5	1.8	<0.31	<0.34	<0.35	<0.33	<0.29
perylene	140	62	30	26	23	22	22	22	22
dibenz[*ah*]anthracene	13[a]	13	2.1[a]	<0.47	<0.66	<0.44	<0.45	<0.46	<0.55
indeno[1,2,3-*cd*]pyrene	76	72	13	3.5	0.49[a]	0.4[a]	<0.4	<0.38	<0.34
benzo[*ghi*]perylene	66	65	16	4.2	<0.34	0.69	0.56	0.65[a]	0.65[a]
total unsubstituted PAHs	855	721	174	63	31	34	34	38	32
C1 naphthalenes	5.0	4.0	1.1	1.3	1.5	1.6	1.0	1.6	1.4
C2 naphthalenes	7.0	4.0	<1.6	<1.0	<0.86	<1.1	<1.2	<1.4	<1.5
C3 naphthalenes	4.0	3.0	<0.55	<0.28	<0.21	<0.28	<0.5	<0.32	<0.49
C4 naphthalenes	<0.02	<0.02	<0.58	<0.37	<0.31	<0.41	<0.44	<0.48	<0.55
C5 naphthalenes	0.6	0.3[a]	<0.49	<0.29	<0.21	<0.3	<0.33	<0.46	<0.4
C1 phenanthrenes/anthracenes	14	13	2.7	0.98	1.2	1.4	1.1	1.0	1.2
C2 phenanthrenes/anthracenes	23	14	<0.21	<0.17	<0.17	<0.19	<0.2	<0.33	<0.18
C3 phenanthrenes/anthracenes	<0.05	8.0	<0.34	<0.27	<0.28	<0.18	<0.25	<0.3	<0.19
C4 phenanthrenes/anthracenes	3.0	8.0	1.7	1.2	0.94	0.89	0.9	1.1	0.94
retene	3.0	8.0	1.7	1.2	0.94	0.89	0.9	1.1	0.94
C5 phenanthrenes/anthracenes	<0.05	<0.05	<0.34	<0.27	<0.23	<0.33	<0.23	<0.48	<1.3
C1 fluoranthenes/pyrenes	48	34	6.2	2.2	0.81	<0.14	0.85	0.56	0.26
C2 fluoranthenes/pyrenes	40	21	6.3	<0.33	<0.3	<0.26	<0.35	<0.31	<0.4
C3 fluoranthenes/pyrenes	<0.07	<0.07	<0.66	<0.3	<0.42	<0.4	<0.34	<0.26	<0.48
C4 fluoranthenes/pyrenes	<0.08	<0.08	<0.72	<0.57	<0.37	<0.56	<0.53	<0.36	<0.53
C5 fluoranthenes/pyrenes	<0.2	<0.2	<0.86	<0.62	<0.66	<0.83	<0.69	<0.85	<0.49
dibenzothiophene	2.0	2.0	<0.18	<0.15	<0.14	<0.16	<0.16	<0.16	<0.16
C1 dibenzothiophenes	1.0	0.9	<0.19	<0.1	<0.09	<0.09	<0.12	<0.16	<0.19
C2 dibenzothiophenes	1.0	1.0	<0.1	<0.08	<0.06	<0.1	<0.12	<0.11	<0.08
2-methylnaphthalene	4.0	2.0	1.0	0.9	1.0	1.0	1.0	1.0	0.9
1-methylnaphthalene	2.0	1.0	<0.9	0.4	0.4	0.5	<0.5	<0.5	<0.4
2,6/2,7-dimethylnaphthalene	3.0	1.0	<1.0	<0.9	<0.7	<1.0	<1.0	<1.0	<1.0
1,2-dimethylnaphthalene	<0.06	<0.08	<2.0	<1.0	<1.0	<1.0	<1.0	<2.0	<2.0
1,4,6/1,3,5/2,3,6-trimethylnaphthalene	1.0	0.7	<0.6	<0.3	<0.2	<0.3	<0.5	<0.3	<0.5
1,2,7/1,6,7/1,2,6/2,3,5-trimethylnaphthalene	0.8	0.6	<0.5	<0.3	<0.2	<0.3	<0.5	<0.3	<0.5
3-methylphenanthrene	3.0	3.0	0.6	<0.2	0.3	0.3	0.2	<0.2	0.2
2-methylphenanthrene	4.0	3.0	1.0	0.3	0.4	0.5	0.4	0.4	0.4
2-methylanthracene	1.0	1.0	<0.3	<0.2	<0.2	<0.2	<0.2	<0.2	<0.2
9-methyl/4-methylphenanthrene + 1-methylanthracene	2.0	3.0	0.6	<0.2	0.2	0.3	0.2	<0.2	0.3
1-methylphenanthrene	2.0	2.0	0.4	<0.2	0.2	0.2	0.2	<0.2	0.2
3,6-dimethylphenanthrene	0.6	0.6	<0.1	<0.09	<0.09	<0.1	<0.1	<0.1	<0.09
9,10-dimethylanthracene	<0.01	<0.01	<0.1	<0.09	<0.09	<0.1	<0.1	<0.1	<0.09
2-methylfluoranthene	9.0	8.0	0.7	0.5	0.2	0.2	0.3	0.1	0.2

[a] Peak detected, but did not meet quantification criteria.

modynamically stable alkyl isomers (*3*, *4*, *27*). This has led to the development of maturation indices based upon C1 phenathrene ratios, in particular. In addition, Bayona et al. (*28*) observed changes in the proportion of monomethyl phenanthrene isomers as a result of microbial degradation. Early diagenesis of anthropogenic PAH in Giltoyees Inlet (top 20 cm) was not accompanied by any consistent trend in the relative proportions (before or after correcting for average natural inputs) of any of the individually analyzed C1 phenanthrenes or anthracenes. However, in the lower core (45−70 cm) the proportion of C1 phenathrenes exhibited a slight increase with increasing depth which may indicate net production of C1 phenanthrenes due to early diagenesis of detrital organic material. There was no significant change ($P > 0.05$) in the proportions of any of the monomethyl phenanthrene isomers in the lower core.

The only obvious change in the fluoranthene/pyrene distribution with depth was the dramatic disappearance of the C2 fluoranthene/pyrene compounds below 15 cm depth, indicating an anthropogenic origin for these compounds. Detailed interpretation of the alkyl-substituted fluoranthene: pyrene ratios in the Giltoyees Inlet core was not attempted, since levels were near or below the detection limits in most cases.

Various workers have demonstrated changes in ratios of specific PAH isomers as a result of weathering by environmental processes (*29*, *30*). In the present work the following ratios increased with increasing sediment depth; (thermo-

dynamic isomer in numerator, see Table 1 for abbreviations) Bper/Ipyr, Pyr/Fln, Bep/Bap; although these changes were not statistically significant ($P > 0.05$). Phen/Anth and Chry/Baa ratios showed no discernible trend. These results, therefore, show only limited evidence for the expected enrichment of thermodynamic isomers with increasing sediment depth. The absence of a discernible trend in these isomer ratios with depth is consistent with data from other sediment cores (*22*, *31*), and further demonstrates the recalcitrance of PAHs in sediments. This recalcitrance may be due to either limited chemical and biological availability of the anthropogenic PAHs in these samples, or increased resistance to biodegradation of PAHs due to rapid onset of anoxia in the sediments.

In summary, changes in the ratios of alkylated to unsubstituted PAH homologues and ratios of thermodynamic to kinetic PAH isomers in the present data set largely reflect changes in the proportion of anthropogenic versus natural inputs. The data do not permit a complete analysis, however, since detailed PAH assignments have not been confirmed for the major portion of the homologue groups. The data show little or no evidence for biodegradation of either natural or anthropogenic PAHs in this sediment core.

Acknowledgments

The Canadian Department of Fisheries and Oceans, and Canadian Department of National Defense are acknowledged for allowing us the use of their research vessels, CSS *Tully* and CFAV *Endeavor*.

Literature Cited

(1) Wakeham, S. G.; Schaffner, C.; Giger, W. *Geochim. Cosmochim. Acta* **1980**, *44*, 415.
(2) Smith, J. N.; Levy, E. M. *Environ. Sci. Technol.* **1990**, *24*, 874.
(3) Radke, M.; Welte, D. H.; Willsch, H. *Geochim. Cosmochim. Acta* **1982**, *46*, 1.
(4) Garrigues, P.; Connan, J.; Parlanti, E.; Bellocq, J.; Ewald, M. *Adv. Org. Geochem.* **1988**, *13*, 1115.
(5) Prahl, F. G.; Carpenter, R. *Geochim. Cosmochim. Acta* **1983**, *47*, 1013.
(6) Maruya, K. A.; Risebrough, R. W.; Horne, A. J. *Environ. Sci. Technol.* **1996**, *30*, 2942.
(7) Kukkonen, J.; Landrum, P. F. *Chemosphere* **1996**, *32*, 1063.
(8) Simpson, C. D.; Mosi, A. A.; Cullen, W. R.; Reimer, K. J. *Sci. Total Environ.* **1996**, *181*, 265.
(9) Cretney, W. J.; Wong, C. S.; Macdonald, R. W.; Erickson, P. E.; Fowler, B. R. *Can. Tech. Rep. Hydrogr. Ocean Sci.* **1983**, *18*, 162.
(10) Paine, M. D.; Chapman, P. M.; Allard, P. J.; Murdoch, M. H.; Minife, D. *Environ. Toxicol. Chem.* **1996**, *15*, 2003.
(11) Naes, K.; Knutzen, J.; Berglind, L. *Sci. Total Environ.* **1995**, *163*, 93.
(12) Thrane, K. E. *Water, Air, Soil Pollut.* **1987**, *33*, 385.
(13) Simpson, C. D.; Cullen, W. R.; Quinlan, K. B.; Reimer, K. J. *Chemosphere* **1995**, *31*, 4143.
(14) Yunker, M. B.; Macdonald, R. W.; Cretney, W. J.; Fowler, B. R.; McLaughlin, F. A. *Geochim. Cosmochim. Acta* **1993**, *57*, 3041.
(15) Simpson, C. D. Ph.D. Dissertation, University of British Columbia, 1997.
(16) Venkatesan, M. I. *Mar. Chem.* **1988**, *25*, 1.
(17) Tan, Y. L.; Heit, M. *Geochim. Cosmochim. Acta* **1981**, *45*, 2267.
(18) Naes, K.; Oug, E. *Environ. Sci. Technol.* **1997**, *31*, 1253.
(19) Bornhold, B. D. *Can. Tech. Rep. Hydrogr. Ocean Sci.* **1983**, *18*, 88.
(20) Venkatesan, M. I. *Mar. Chem.* **1987**, *21*, 267.
(21) Sanders, G.; Jones, K. C.; Hamilton-Taylor, S.; Dorr, H. *Environ. Pollut.* **1995**, *89*, 17.
(22) Van Zoest, R.; Van Eck, G. T. M. *Mar. Chem.* **1993**, *44*, 95.
(23) Roques, D. E.; Overton, E. B.; Henry, C. B. *J. Environ. Qual.* **1994**, *23*, 851.
(24) Venosa, A. D.; Suidan, M. T.; Wrenn, B. A.; Strohmeier, K. L.; Haines, J. R.; Eberhart, B. L.; King, D.; Holder, E. *Environ. Sci. Technol.* **1996**, *30*, 1764.
(25) Jacquot, F.; Guiliano, M.; Doumenq, P.; Munoz, D.; Mille, G. *Chemosphere* **1996**, *33*, 671.
(26) Ehrhardt, M. G.; Burns, K. A.; Bicego, M. C. *Mar. Chem.* **1992**, *37*, 53.
(27) Kawaka, O. E.; Simoneit, B. R. T. *Org. Geochem.* **1994**, *22*, 947.
(28) Bayona, J. M.; Albaiges, J.; Solanas, A. M.; Pares, R.; Garrigues, P.; Ewald, M. *Int. J. Environ. Anal. Chem.* **1986**, *23*, 289.
(29) Aceves, M.; Grimalt, J. O. *Atmos. Environ.* **1993**, *27B*, 251.
(30) Gschwend, P. M.; Hites, R. A. *Geochim. Cosmochim. Acta* **1981**, *45*, 2359.
(31) Eganhouse, R. P.; Gosset, R. W. *Processes and Analytical* In *Organic Substances in Sediments and Water*; Baker, R. A., Ed.; Lewis Publishers: Boca Raton, FL, 1991; Vol. 2, pp 191−220.

Received for review May 14, 1997. Revised manuscript received July 8, 1998. Accepted July 15, 1998.

ES970419Y